Randomized Animal Trial

Down-Regulation of Insulin Signaling Is Involved in Painful Diabetic Neuropathy in Type 2 Diabetes

Zhen-Zhen Kou, MD, PhD[1], Chun-Yu Li, BS[1], Jun Tang, MD[2], Jia-Chen Hu, BS[1], Juan Qu, MD[1, 3], Yong-Hui Liao, MD[1], Sheng-Xi Wu, MD, PhD[1], Hui Li, MD, PhD[1] and Yun-Qing Li, MD, PhD[1]

From: [1]Department of Anatomy, Histology and Embryology, K.K. Leung Brain Research Centre, The Fourth Military Medical University, Xi'an, China. [2]Department of Anesthesiology, School of Stomatology, The Fourth Military Medical University, Xi'an, China. [3]Department of Otolaryngology, Xijing Hospital, The Fourth Military Medical University, Xi'an, PR China.

Address Correspondence: Yun-Qing Li, PhD. Professor and Director, Department of Anatomy, Histology and Embryology, K.K.Leung Brain Research Centre, The Fourth Military Medical University, No. 169 West Changle Road, Xi'an 710032, PR China E-mail: deptanat@fmmu.edu.cn

Background: Previous theories considered that the main cause of painful diabetic neuropathy (PDN) was due to hyperglycemia. However, recent evidence indicated that hyperinsulinemia plays a greater role in type 2 diabetic metabolisms (T2DM).

Objectives: Our aim was to explore insulin signaling to determine the molecular mechanism involved in the pathogenesis of PDN in T2DM.

Study Design: A randomized, double blind, controlled animal trial.

Methods: We observed the localization of insulin receptor (IR) and phosphorylated insulin receptor substrate 1 (IRS-1) in the spinal cord using in situ hybridization and immunohistochemistry. Then we investigated the alternations of IR and pIRS-1 and the activity of the JAK2/STAT3 pathway by immunohistochemistry, Western Blotting, and cell culture. Finally, we detected the influence of intrathecal JAK2/STAT3 inhibitor (AG490) on nociceptive behavior and insulin signaling in ob/ob mice using Western Blotting.

Results: We found that IR and pIRS-1 are mainly located in neurons in the superficial layer of the spinal dorsal horn. The expressions of IR and pIRS-1 decreased and the JAK2/STAT3 pathway activated in the spinal dorsal horn in ob/ob mice with mechanical hyperalgesia. Next, our *in vitro* results indicated that hyperinsulinemia and hyperglycemia impaired insulin signaling along with the activated JAK2/STAT3 pathway in differentiated human neuronal cells (SH-SY5Y). Treatment through intrathecal injection of AG490, an inhibitor of the JAK2/STAT3 pathway, alleviated mechanical hyperalgesia in ob/ob mice and prevented impaired insulin signaling in the spinal cord.

Limitations: The activation of the JAK2/STAT3 pathway could not explain the mechanism of PDN in T1DM.

Conclusions: We demonstrate that insulin signaling impairment in the spinal dorsal horn is associated with the activated JAK2/STAT3 pathway, which contributes to the progressive PDN in T2DM.

Key words: Painful diabetic neuropathy, mouse, insulin receptor, insulin receptor substance 1, JAK2, STAT3

Pain Physician 2013; 16:E71-E83

P ainful diabetic neuropathy (PDN) is one of the most common complications in the early to intermediate stages of diabetes mellitus (DM) (1). Both diabetic patients and animal models frequently exhibit increased responsiveness to nociceptive stimuli (2-5). The management of PDN is challenging because although such pain could be alleviated through drugs or electrical spinal-cord stimulation, the development of diabetic neuropathy is generally progressive. Previous research focused much attention on the

peripheral nerve and its sensory endings and supported them as impulse generators in PDN. Recent evidence demonstrated that the central nervous system (CNS) plays a critical role in PDN (3,6), but the underlying mechanisms remain poorly understood. It has been shown that nociceptive signals are conveyed to the CNS for integration, beginning in the spinal cord (7). Thus, to investigate the molecular and cellular bases in the spinal cord is essential for understanding the mechanisms of PDN.

There are 2 main types of DM: type 1 DM (T1DM) and type 2 DM (T2DM). The T1DM is known as insulin deficiency, while the T2DM, representing 90% of the diabetic population, is the hyperinsulinemia. Therefore, in spite of sharing nociceptive behavior in both T1DM and T2DM, the mechanism of PDN in the T2DM might be quite different from the T1DM. However, there are few reports about the specific mechanisms of PDN in the T2DM.

It has been demonstrated that the insulin receptor (IR) is abundant in the CNS, with particularly high concentrations in neurons (8,9). In rodents, IRs are selectively distributed in the cerebral cortex, hippocampus, and spinal cord. In the T2DM, the deficiency of insulin signaling in the cerebral cortex and hippocampus exert a negative influence on learning and memory (10). Therefore, we hypothesized that insulin signaling in the spinal cord may also play a role in PDN of T2DM.

The interaction between CNS insulin signaling and the Janus kinase (JAK)/signal transducer and activator of transcription (STAT) pathway has been addressed (11-13). The JAK/STAT pathway participates in many cellular processes, including cell survival, proliferation, differentiation, development, and inflammation. Of the 4 JAK isoforms and 7 STAT isoforms known, JAK2 and STAT3 are highly expressed in the CNS. Chronic hyperinsulinemia was shown to activate the JAK2/STAT3 pathway, accompanied with impaired insulin signaling in diabetic nephropathy and resulted in the suppression of hepatic glucose output (14-16). Recent reports also demonstrated that the JAK2/STAT3 pathway has neuronal specific functions in synaptic plasticity (17,18). Thus, these observations raise the possibility that the JAK2/STAT3 pathway may interact with insulin signaling in PDN.

OBJECTIVES

Based on these considerations, we sought to detect the changes of IR and phosphorylated insulin receptor substrate 1 (pIRS-1) and the potential role of the JAK2/STAT3 pathway in PDN of T2DM.

METHODS

Experimental Animals

All animal procedures were approved by the Animal Care and Use Committees of the Fourth Military Medical University, and carried out in accordance with the Principles of Laboratory Animal Care (NIH Publication no. 85-23, revised 1985). Male ob/ob mice (B6.V-Lepob/J) and their lean littermates (ob/-) at 8, 12, and 16 weeks of age were used (Jackson Laboratories, Bar Harbor, ME, USA). For the type 1 diabetic animal model, male Sprague-Dawley rats weighing 220 - 250 g bought from Laboratory Animal Resources of the Fourth Military Medical University were utilized and injected with a single intraperitoneal injection of 60mg/kg streptozotocin (STZ, Sigma, St. Louis, MO, USA), which was freshly dissolved in ice-cold sodium citrate (pH 4.5). The diabetes was confirmed on the third day by measurements of blood glucose concentrations in samples obtained from the tail vein. Only rats with blood glucose concentrations of > 20 mM were further used. All animals were housed in standard conditions (12 hours light/dark cycles) with water and food available ad libitum. In order to keep comparability, all behavior experiments were performed during the morning (9:00 –11:00 am).

Cell Culture and Stimulation

SH-SY5Y human neuroblastoma cells (ATCC, Manassas, VA, USA) were grown in DMEM (Dulbecco's modified Eagle's medium) supplemented with 10% heat-inactivated fetal calf serum, 100 units/ml penicillin, and 100 μg/ml streptomycin in 5% CO_2 atmosphere at 37°C. Differentiated cells were used after 15 days of retinoic acid (RA, Sigma, St. Louis, MO, USA) treatment. The effects of insulin (Sigma, St. Louis, MO, USA) and glucose (Anresco Laboratories, San Francisco, CA, USA) on the differentiated SH-SY5Y were examined. Briefly, serum-starved cells were incubated for 16 hours at 37°C in serum-free DMEM, and then stimulated with insulin (100 nM) and different concentrations of glucose (25 mM, 125 mM) for 16 hours. After stimulation, cells were harvested by rinsing in ice-cold Phosphate Buffered Saline (PBS) and scraping into a lysis buffer containing a protease inhibitor cocktail and phosphatase inhibitors for 30 minutes. Then, the insoluble materials were removed by centrifugation (12000 g at 4°C, for 15 minutes), and protein concentrations were determined using a protein assay kit (Pierce Chemical Company, Rockford, IL, USA).

Measurement of Hindpaw Withdrawal Threshold

Experiments were performed on the ob/ob mice and STZ-treated rats with their age-matched controls, respectively. To quantify the mechanical sensitivity of the hindpaw, animals were placed in individual plastic boxes and allowed to acclimate for 30 min. A series of calibrated von Frey filaments (Stoelting, Kiel, WI, USA) were applied to the plantar surface of the hindpaw (ranging from 0.4 g to 60.0 g for rat and from 0.02 g to 2.0 g for mouse) with a sufficient force to bend the filaments for 5 seconds or until paw withdraw. In the presence of a response, the filament of the next lower force was applied. In the absence of a response, the filament of the next greater force was applied. A positive response was indicated by a sharp withdrawal of the paw. Each filament was applied 10 times and the minimal value which caused at least 6 responses was recorded as the paw withdrawal thresholds (PWTs). All behavioral studies were performed under blind conditions.

In Situ Hybridization

After deeply anaesthetizing 3 normal mice with an intraperitoneal injection of pentobarbital (5 mg/100 g for mice), we perfused them with 80 ml of 4% (w/v) formaldehyde in 0.1 M PB as a fixative and post-fixed the spinal cord overnight at 4°C for 4 hours. After which, we placed the tissues in 30% (w/v) sucrose in PBS at 4°C for 10 – 12 hours, and the spinal cord was cut into 25 μm thick transverse sections on a freezing microtome. All steps of insulin receptor mRNA in situ hybridization were performed following insulin receptor mRNA in situ hybridization kit protocols (Boster Inc., Wuhan, China) with the DNA probe sequences as 5'-ACGTT TGAGG AT-TAC CTGCA CAACG TGGTT-3', 5'-GACCA TGCCT GAAGC CAAGG CTGAT GACAT-3' and 5'-ATGCG CATGT GCTGG CAATT CAACC CCAAG-3'. Negative controls were treated with RNase before hybridization following the instructions of the Boster in situ hybridization kit.
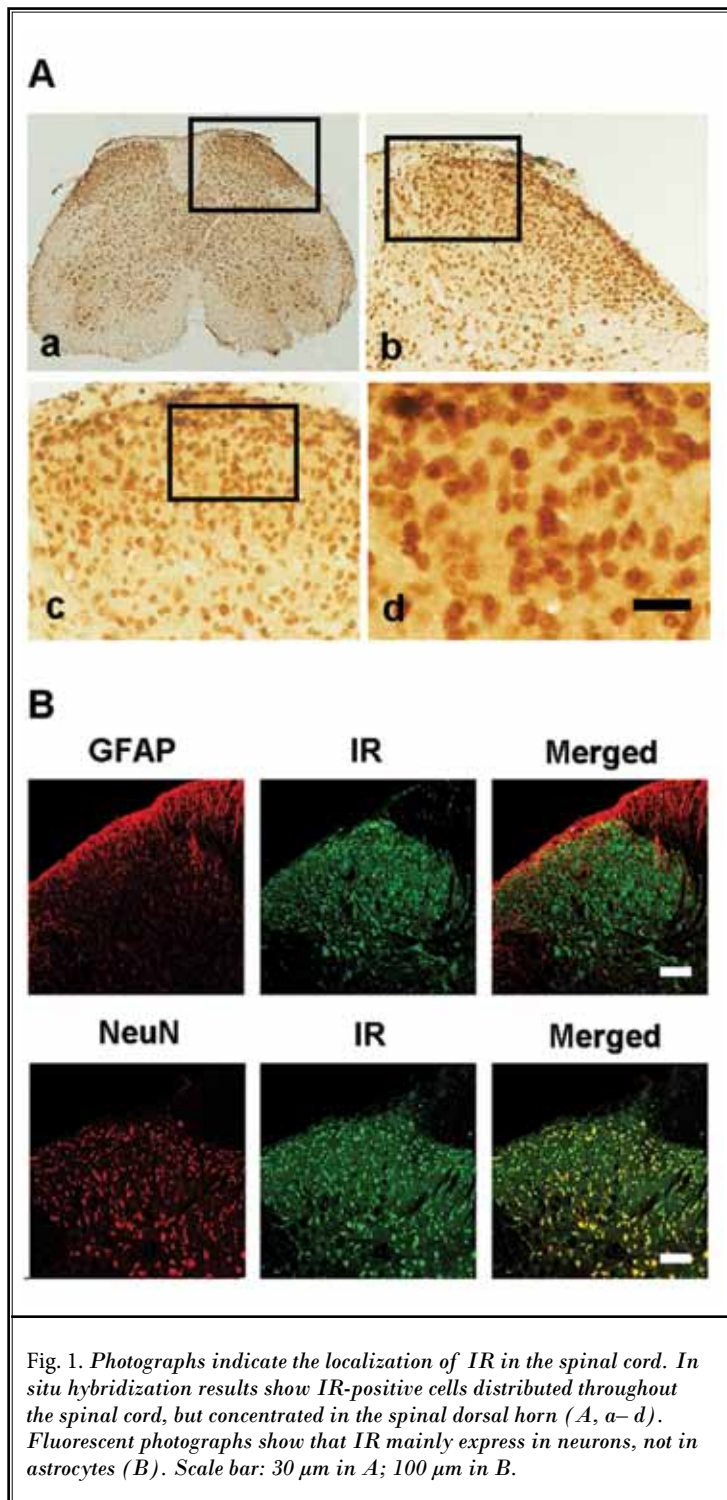
Immunohistochemistry

The animals were deeply anaesthetized with an injection of pentobarbital and perfused for immunohistochemistry (5 mg/100 g for mice, 100 mg/kg for rats). The lumbar segments of the spinal cord were removed, post-fixed at 4°C for 4 hours, and placed in 30% (w/v) sucrose solution for 24 hours at 4°C. Transverse spinal cord sections (25 μm) were incubated in a blocking solution (5% v/v normal goat serum) for one hours at room temperature and then incubated for 48 hours at 4°C with primary antibodies: anti-insulin receptor (rabbit polyclonal, 1:1000; Abcam, Cambridge, MA, UK), anti-phosphorylated-insulin receptor substance 1 (Ser302, mouse polyclonal, 1:500; Boster Inc., Wuhan, China), anti-GFAP (mouse monoclonal, 1:1000; Chemicon, Temecula, CA, USA), anti-NeuN (mouse monoclonal, 1:2000; Chemicon), anti-phosphorylated-JAK2 (Tyr1007/1008, rabbit monoclonal, 1:1000; Abcam), and anti-phosphorylated-STAT3 (Tyr705, rabbit monoclonal, 1:1000; Cell Signaling Technology, Beverly, MA, USA). Following incubation, the sections were incubated with species-specific secondary antibodies for 6 hours in solutions containing Alexa488-conjugated donkey anti-mouse IgG (1:500; Invitrogen, Carlsbad, CA, USA) and Alexa594-conjugated donkey anti-guinea pig IgG (1:500; Invitrogen). Finally, the sections were rinsed with PBS, mounted onto clean glass slides, air-dried, and cover slipped with a mixture of 0.05 M PBS containing 50% (v/v) glycerin and 2.5% (w/v) triethylenediamine. The sections were observed under a confocal laser scanning microscope (FV-1000, Olympus, Tokyo, Japan). The images were captured and analyzed with Fluoview 1000 (Olympus).

Western Blotting

The animals were killed by decapitation under pentobarbital anesthesia (n = 6 in each group). The lumbar spinal dorsal horn was homogenized in a lysis buffer containing proteinase inhibitors and phosphatase inhibitors as described. Equal samples of protein from cells and animals were electrophoresed by SDS-PAGE in 10% polyacrylamide gel and transferred to PVDF membranes (Millipore, Bedford, MA, USA). The membranes were blocked with 5% bovine serum albumin (BSA) and incubated overnight at 4°C with primary antibodies, including anti-IR, anti-NeuN, anti-pJAK2, anti-pSTAT3, anti-STAT3 (rabbit monoclonal, 1:1000; Cell Signaling Technology), anti-JAK2 (rabbit monoclonal, 1:1000, Cell Signaling Technology), anti-pIRS-1 (Ser302, rabbit polyclonal, 1:1000; Cell Signaling Technology), and anti-β-actin (mouse monoclonal, 1:2000; Sigma). After incubation of the membrane with peroxidase-conjugated anti-rabbit secondary antibodies (Santa Cruz Biotechnology, Santa Cruz, CA, USA) for 2 hours at room temperature, the reaction products were visualized with enhanced chemiluminescence (Amersham Life Science, Amersham, UK). Western blots were made in triplicate. Band density was measured and normalized against a loading control band.

Fig. 1. *Photographs indicate the localization of IR in the spinal cord. In situ hybridization results show IR-positive cells distributed throughout the spinal cord, but concentrated in the spinal dorsal horn (A, a–d). Fluorescent photographs show that IR mainly express in neurons, not in astrocytes (B). Scale bar: 30 µm in A; 100 µm in B.*

Intrathecal Implantation and Drug Administration

Intrathecal implantation was performed by inserting polyethylene (PE) tubing to inject the drug directly into the subarachnoid space of the lumbar enlargement. Briefly, under pentobarbital anesthesia, a pre-measured length of PE-10 tubing was inserted caudally into the lumbar enlargement (lumbar spinal segment L4-L6) through a midline incision at the back of the mouse at the level of the lumbar vertebra and into the subarachnoid space. The external part of the catheter was tied in a loose knot and tunneled subcutaneously in the back. Three days after catheterization, the catheter placement was verified by the observation of hind limb paralysis after intrathecal injection of 0.1 % lidocaine (10 µl). Only mice displaying paralysis by lidocaine were included in the experiments. Two days after the lidocaine test, mice at the age of 8 weeks were injected with either a JAK2/STAT3 pathway inhibitor (AG490, 10 nmol/10 ml, Sigma) or saline of 10 µl through the catheter at 10:00 - 10:30 am every day for 3 days.

Statistical Analysis

The results from immunohistochemistry were calculated as detailed in a previous report (19). Analysis of the time-course of the nociceptive behavior test between saline- and drug-treated groups was performed by 2 factors (group and times) with repeated measures analysis of variance (ANOVA). Data were expressed as mean ± SD and were analyzed by SPSS 16.0 (SPSS Inc., Chicago, IL, USA). The differences between groups were considered as statistically significant at a value of $P < 0.05$.

Results
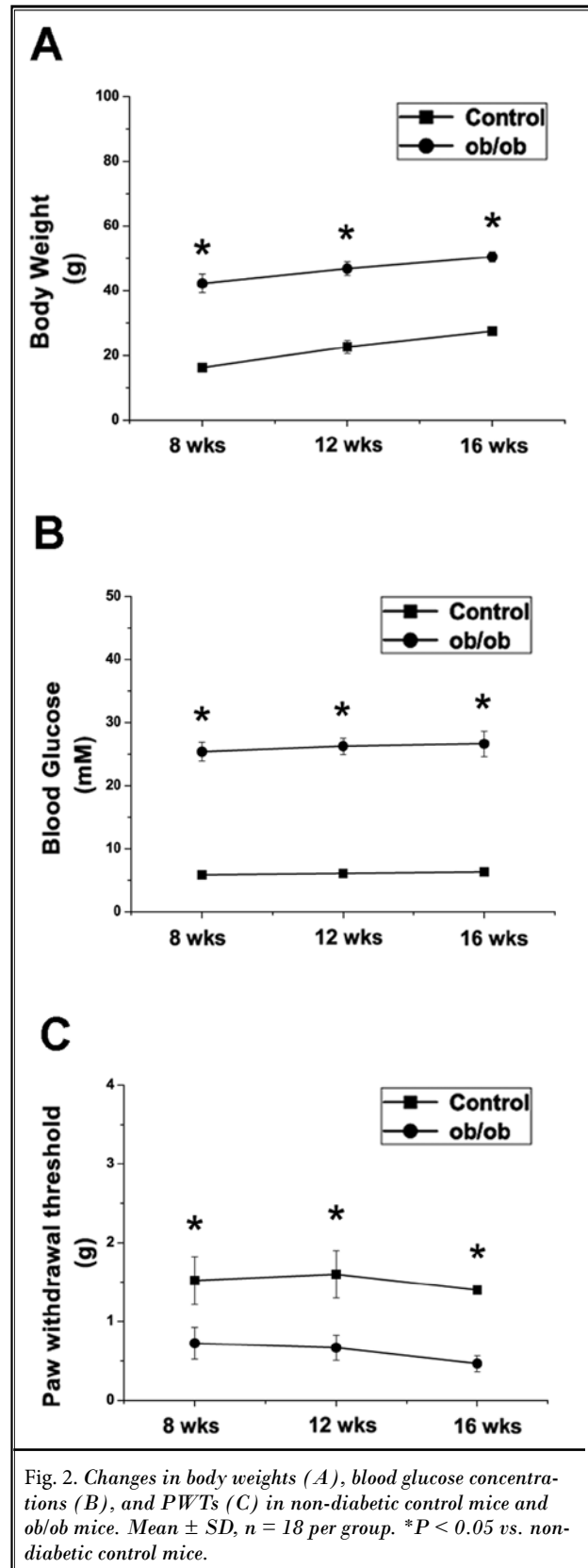
Distribution of IR in the Spinal Cord

To visualize the distinct localization of IR in the spinal cord, we performed in situ hybridization and immunohistochemistry. Our results showed that IR mRNA was widely expressed in both the grey matter and the white matter of the lumbar spinal cord. However, the highest density of IR mRNA signals was revealed in the superficial layer of the spinal dorsal horn, laminae I and II, considered the

fundamental area in nociceptive transmission in the CNS (Fig. 1A). Consistent with in situ hybridization, fluorescent immunostainings with the IR antibody indicated that the IR-positive cells were evident in the grey matter of the dorsal horn (Fig. 1B). To define the cell type of IR-positive cells, we conducted double-immunolabellings with cell type-specific markers (NeuN for neuron, GFAP for astrocyte), respectively (Fig. 1B). In the superficial layer of the spinal cord, 93.9% of IR-positive products co-expressed with NeuN. These results suggested that the IR are mainly located in the neurons of the spinal dorsal horn.

Changes of IR and pIRS-1 in the Spinal Dorsal Horn of ob/ob Mice in PDN

To investigate whether insulin signaling located at the spinal dorsal horn is involved in PDN, we measured physiological parameters and PWTs. In parallel with elevated blood glucose levels and body weights, ob/ob mice developed mechanical hyperalgesia when tested with von Frey filaments (Fig. 2, $P < 0.05$). As demonstrated in Fig. 2C, compared with controls, the mechanical PWTs decreased substantially in ob/ob mice at the age of 8 weeks (0.72 ± 0.20 g, n = 6), and remained at the reduced level for another 8-week test period (0.67 ± 0.16 g at 12 weeks, 0.47 ± 0.10 g at 16 weeks).

To determine the changes of IR and pIRS-1 with the progressive mechanical hyperalgesia, the protein expressions were examined. In immunohistochemistry, the results showed that compared with the control mice, the number of IR-positive cells decreased from 8-weeks-old (86% of control) to 16-weeks-old group (57% of control) in ob/ob mice (Fig. 3A and B, $P < 0.05$). Apparent differences in the numbers of IR/NeuN colocalized neurons between ob/ob mice and the controls were also shown (Fig. 3A and C, $P < 0.05$). In addition, we also confirmed that pIRS-1-positive cells were present in the spinal dorsal horn, and pIRS-1 immunoreactivities were detected in most IR-positive cell bodies and processes (Fig. 3D and E). Western blotting also confirmed the alternations of IR, NeuN, and pIRS-1 in the spinal dorsal horn (Fig. 3F). Normalized to the densitometry values of β-actin in each sample, data obtained here indicated a significant decrease in IR expressions of ob/ob mice from 8 to 16 weeks of age (Fig. 3F and G, $P < 0.05$). Moreover, analysis showed that compared with the controls, the levels of pIRS-1 reduced in ob/ob mice (Fig. 3F and H, $P < 0.05$). In contrast, the number of neurons of ob/ob mice was unchanged (Fig. 3A, F and I, $P > 0.05$). These results suggested that the decreases of
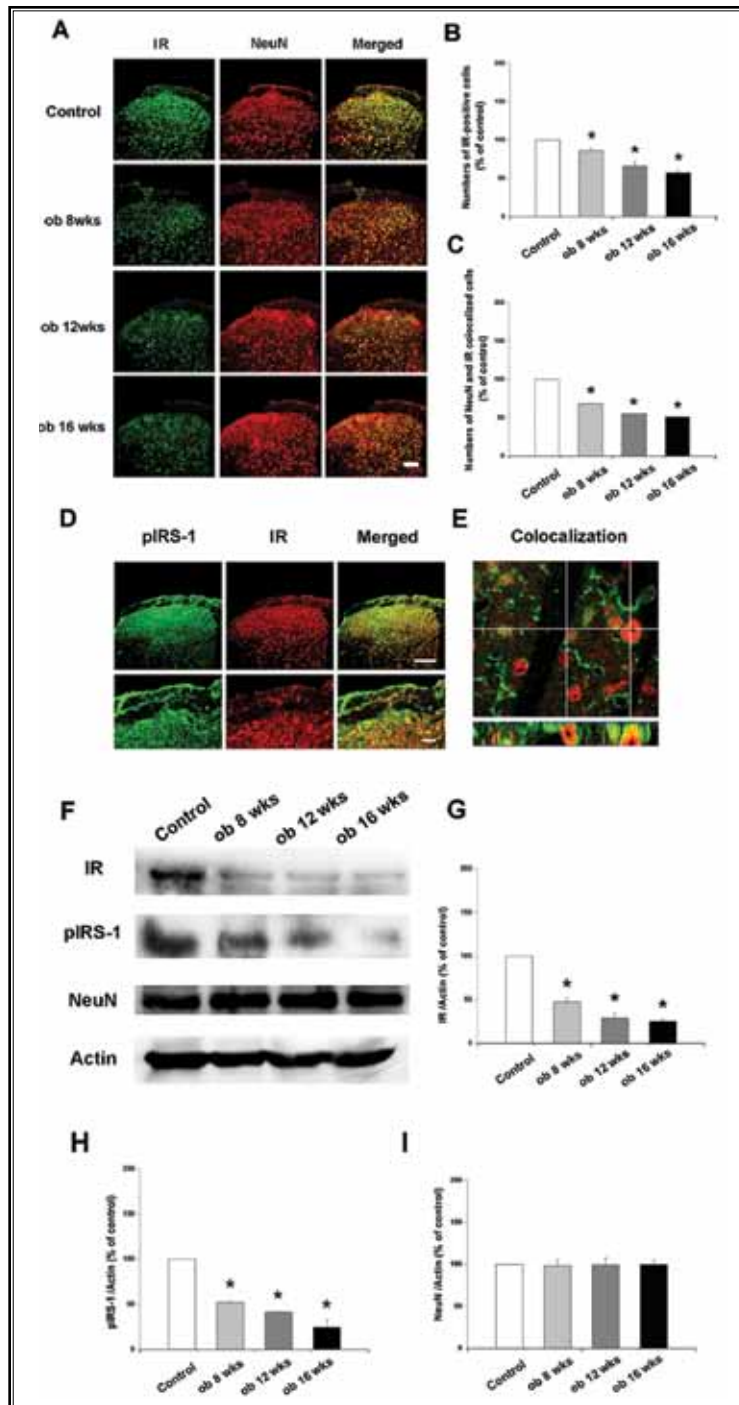

Fig. 2. *Changes in body weights (A), blood glucose concentrations (B), and PWTs (C) in non-diabetic control mice and ob/ob mice. Mean ± SD, n = 18 per group. *P < 0.05 vs. non-diabetic control mice.*

Fig. 3. *Expressions of IR are reduced but NeuN is unaffected in the spinal dorsal horn of ob/ob mice (A), scale bar = 30 μm. Statistical analysis of the numbers of IR-positive cells (B) and NeuN/IR colocalized cells (C) in different groups. The pIRS-1-positive elements concentrate in the spinal dorsal horn and colocalize with IRs (D). Representative confocal z-stack digital image of double-immunolabelled with pIRS-1 (green) and IR (red) are shown (E). Scale bar: 100 μm in upper panel, 30 μm in lower panel. The blots show the changes of IR, pIRS-1, and NeuN (F). Statistical analysis of the expressions of IR (G), pIRS-1 (H), and NeuN (I) in different groups. The sample of the control group is set as 100%. Mean ± SD, n = 6 per group. *P < 0.05 vs. non-diabetic control mice.*

IR and pIRS-1 in the spinal dorsal horn were consistent with the progressive mechanical hyperalgesia in ob/ob mice, but the neuronal numbers were unaffected.

Changes of JAK/STAT3 Pathway Activation in the Spinal Dorsal Horn of ob/ob Mice in PDN

We next tested the JAK2/STAT3 pathway in ob/ob mice. To this end, we first performed double-immunolabellings for pJAK2/pIRS-1 in the spinal dorsal horn. Our results showed that the specific labeling of pIRS-1 colocalized with pJAK2 were usually restricted to the neuronal perikarya and processes (Fig. 4A). Moreover, results from Western blotting indicated that the levels of pJAK2 and pSTAT3 in the spinal dorsal horn increased significantly in ob/ob mice (Fig. 4B, C and D, $P < 0.05$), but the total JAK2 and total STAT3 were unchanged (Fig. 4E and F, $P > 0.05$).

To determine whether the activation of the JAK2/STAT3 pathway is specific in the T2DM, we detected the activation of JAK2 and STAT3 in the spinal dorsal horn of STZ-induced diabetic rats as well. Following a single intraperitoneal injection of STZ, we monitored the blood glucose, body weight, and PWTs for 4 weeks. Along with elevated blood glucose levels, the STZ rats developed mechanical hyperalgesia from 2 weeks but peaked at 4 weeks when tested with von Frey filaments (Fig. 5A, B and C, $P < 0.05$). The relative levels of the pJAK2 and pSTAT3 were presented in Fig. 5D, indicating there was no remarkable difference (Fig. 5E and F). Taken together, these results suggested a specific role of the JAK2/STAT3 pathway in the spinal dorsal horn in T2DM, but not in T1DM.

The Effects of Chronic Insulin and High Glucose Treatment in SH-SY5Y Cells

We used differentiated SH-SY5Y cells, which expressed endogenous insulin signaling and the JAK2/STAT3 pathway, to examine the effects of glucose and insulin treatments (Fig. 6A). As shown in Fig. 6B, in the presence of insulin treatment for 16 hours, the IR decreased significantly in the cells (Figs. 6B and
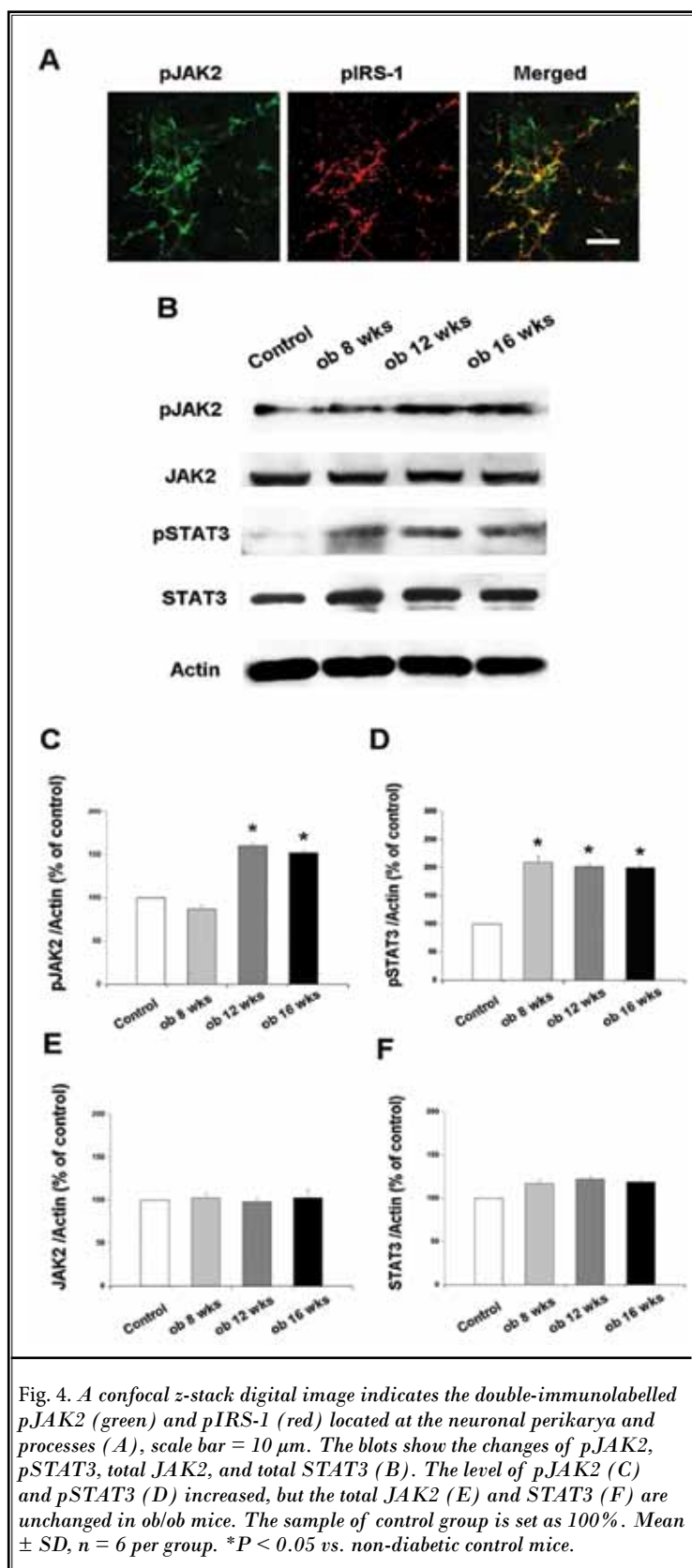
C, $P < 0.05$). In pIRS-1 levels, after exposed to high concentrations of glucose (125 mM) and insulin (100 nM) respectively, the pIRS-1 was significantly decreased. Moreover, when cells were treated with insulin and glucose together for 16 hours, pIRS-1 levels reduced significantly (Figs. 6B and D, $P < 0.05$). The levels of pJAK2 and pSTAT3 could be increased by 100 nM insulin but not in response to 125 mM glucose. The presence of glucose and insulin together could activate the JAK2/STAT3 pathway significantly, independent of the dose of glucose (Figs. 6E and F, $P < 0.05$). These results demonstrated that chronic hyperinsulinemia treatment is responsible for the reduction of IR and pIRS-1. Furthermore, the hyperinsulinemia is sufficient to activate the JAK2/STAT3 pathway independent of the concentration of glucose.
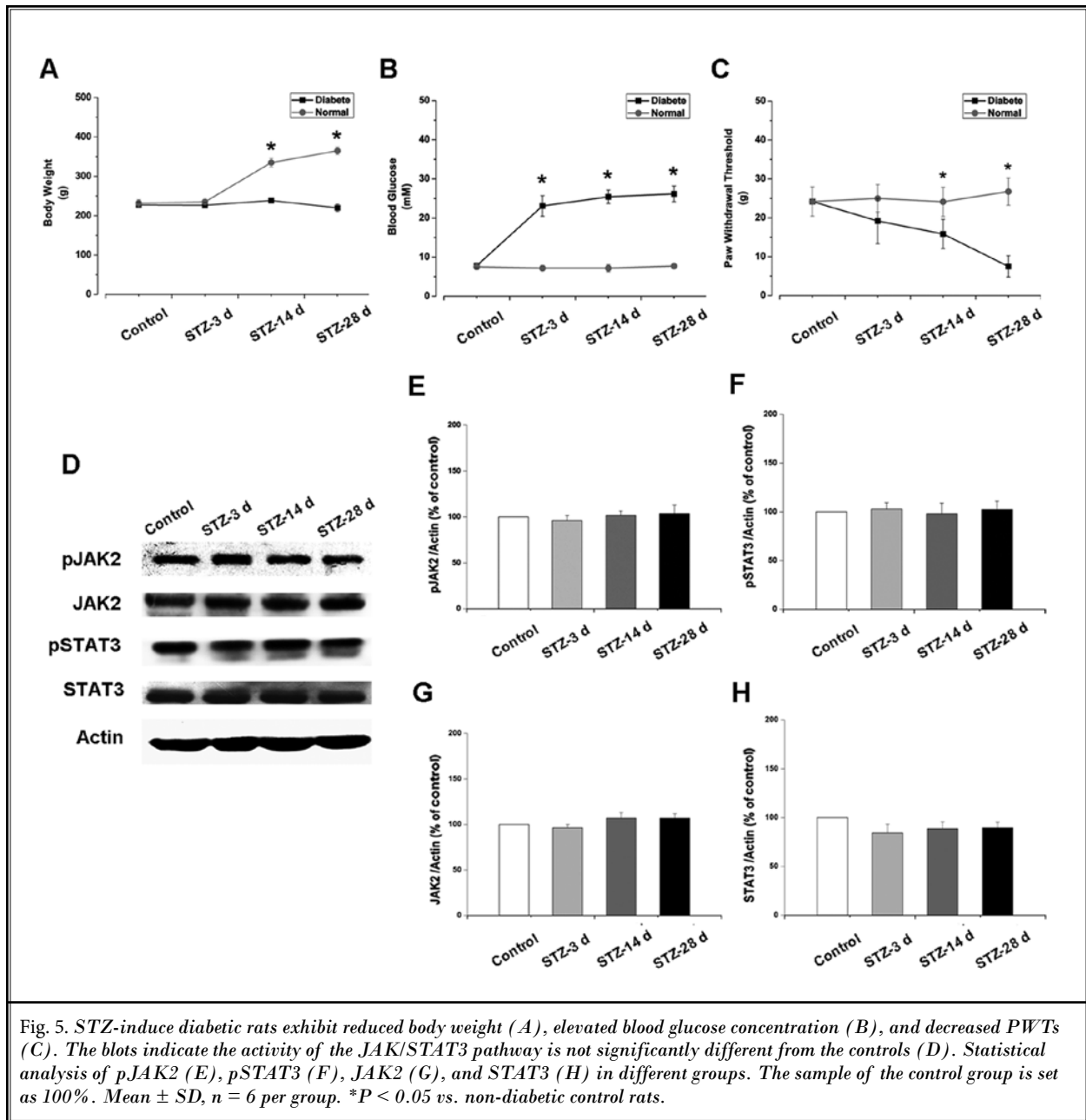
The Role of the JAK2/STAT3 Pathway in PDN and Impaired Insulin Signaling

We administered an inhibitor of the JAK2/STAT3 pathway, AG490, to explore the role of the JAK2/STAT3 pathway in PDN and to determine whether it contributed to the impaired insulin signaling *in vivo*. After the administration, the behavior results demonstrated that the PWTs of the ob/ob mice treated with AG490 elevated significantly more than the ob/ob mice treated with saline (Fig. 7A, $P < 0.05$). We found that intrathecal administration of AG490 effectively reduced the levels of pJAK2 and pSTAT3 (Fig. 7B, E, and F, $P < 0.05$). Notably, the decreasing tendency of IR and pIRS-1 expressions is attenuated after AG490 treatment (Fig. 7B, C, and D, $P < 0.05$), suggesting that AG490 produced an influence on recovering the insulin signaling in spinal cord. Overall, we found out that the JAK2/STA3 pathway is involved in PDN and an underlying mechanism in insulin signaling impairment in ob/ob mice.

DISCUSSION

Although STZ-diabetic rodents (T1DM) with hypoinsulinemia were used widely

Fig. 4. *A confocal z-stack digital image indicates the double-immunolabelled pJAK2 (green) and pIRS-1 (red) located at the neuronal perikarya and processes (A), scale bar = 10 μm. The blots show the changes of pJAK2, pSTAT3, total JAK2, and total STAT3 (B). The level of pJAK2 (C) and pSTAT3 (D) increased, but the total JAK2 (E) and STAT3 (F) are unchanged in ob/ob mice. The sample of control group is set as 100%. Mean ± SD, n = 6 per group. *P < 0.05 vs. non-diabetic control mice.*

Fig. 5. *STZ-induce diabetic rats exhibit reduced body weight (A), elevated blood glucose concentration (B), and decreased PWTs (C). The blots indicate the activity of the JAK/STAT3 pathway is not significantly different from the controls (D). Statistical analysis of pJAK2 (E), pSTAT3 (F), JAK2 (G), and STAT3 (H) in different groups. The sample of the control group is set as 100%. Mean ± SD, n = 6 per group. *P < 0.05 vs. non-diabetic control rats.*

for studying PDN, the main limitation with this model is that it only represents 10% of the diabetic population. Thus, in our study, mice homozygous for the obese spontaneous mutation (Lep[ob] commonly referred as ob/ob) exhibit obesity, hyperglycemia, and hyperinsulinemia, display mechanical hyperalgesia from the age of 8 to 16 weeks, and as such are an appropriate animal model for studying the mechanism of PDN in the T2DM (4,20).

Despite much progress in understanding the influence of chronic hyperinsulinemia and reduced insulin effectiveness on diabetes (21), little is known about the role of insulin signaling in the spinal cord, particularly in PDN, a common complication in diabetic patients. In the present study, our detailed immunohistochemistry analyses provided evidence that most IRs were found in neurons and distributed densely in the superficial layer of the spinal dorsal horn, which has been implicated in
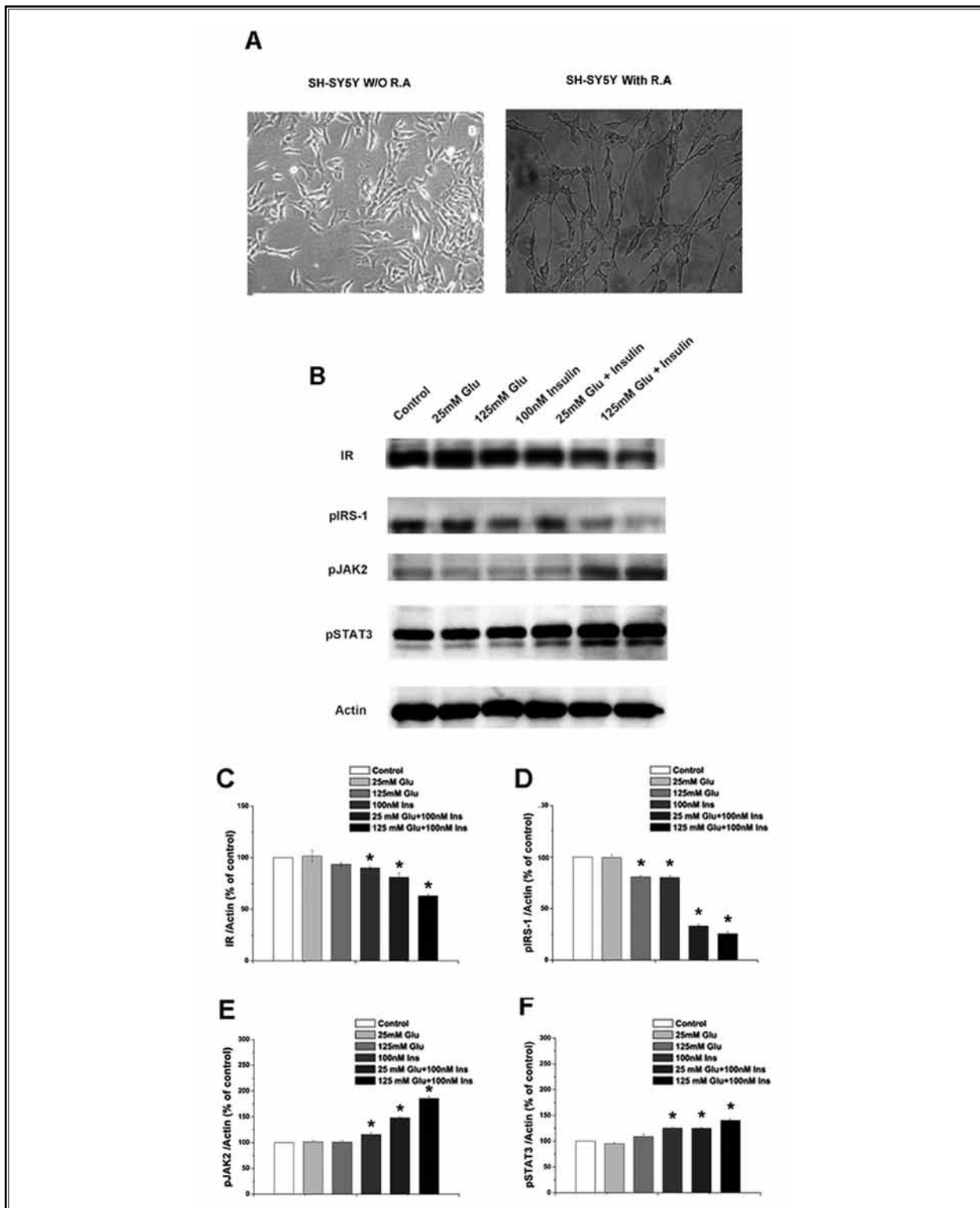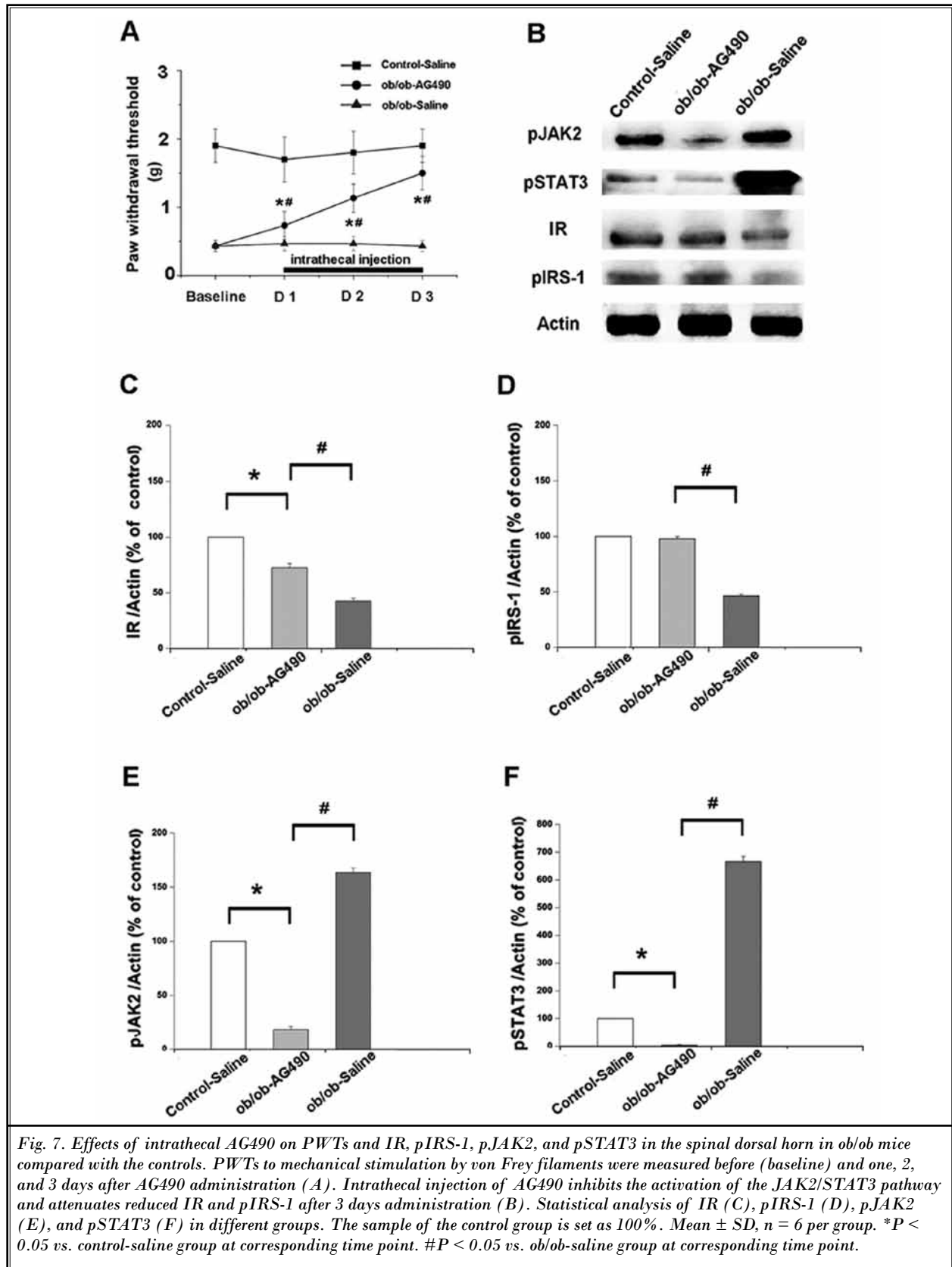
Fig. 6. *Effects of chronic glucose and insulin treatments on IR, pIRS-1, pJAK2, and pSTAT3 in differentiated SH-SY5Y cells. Cells were cultured without (W/O) or with 10 mM RA, a high percentage of cells show a clear morphological differentiation after 15 days RA treatment (A). The blots show the changes of IR, pIRS-1, and the JAK2/STAT3 pathway activation after different treatments for 16 hours (B). Statistical analysis of IR (C), pIRS-1 (D), pJAK2 (E), and pSTAT3 (F) in different groups. The sample of the control group is set as 100%. Mean ± SD, n = 6 per group. *P < 0.05 vs. untreated control group.*

Fig. 7. Effects of intrathecal AG490 on PWTs and IR, pIRS-1, pJAK2, and pSTAT3 in the spinal dorsal horn in ob/ob mice compared with the controls. PWTs to mechanical stimulation by von Frey filaments were measured before (baseline) and one, 2, and 3 days after AG490 administration (A). Intrathecal injection of AG490 inhibits the activation of the JAK2/STAT3 pathway and attenuates reduced IR and pIRS-1 after 3 days administration (B). Statistical analysis of IR (C), pIRS-1 (D), pJAK2 (E), and pSTAT3 (F) in different groups. The sample of the control group is set as 100%. Mean ± SD, n = 6 per group. *P < 0.05 vs. control-saline group at corresponding time point. #P < 0.05 vs. ob/ob-saline group at corresponding time point.

nociceptive transmission. In addition, IR activation is coupled with signal transduction pathways via the IRS family. The IRS-1 has been identified playing an essential role in insulin signaling transduction in the CNS (22). However, it was reported that in ventral hypothalamic nuclei, IRS-1 did not concentrate where IR were found, indicating a restricted distribution and function (23). But our findings showed that in the spinal dorsal horn, pIRS-1 expressed distinctly in IR-positive neurons, suggesting IRS-1 is the primary cytosolic substrate of IR in spinal insulin action. Importantly, by detecting the IR and pIRS-1 expressions, we determined the reduced insulin signaling in the spinal dorsal horn of ob/ob mice, which was consistent with the development of mechanical hyperalgesia from the age of 8 to 16 weeks. Collectively, these results indicate down-regulation of insulin signaling in line with the progressive PDN in ob/ob mice.

The next stage was to consider why insulin signaling impairment existed in the spinal dorsal horn in PDN. Although insulin action has been indicated, a number of signaling cascades such as the JAK2/STAT3 pathway may interact with insulin signaling in neuronal functions in the CNS, but remain unclear in PDN (24,25). We found that pJAK2 and pIRS-1 colocalized in neuronal perikarya and processes in the spinal dorsal horn, which was consistent with previous report in the hippocampus (18). However, there are conflicting reports about the localization of JAK2 and STAT3 in different cell types (17,26-28). This might be explained by the following reasons. First, these previous studies tested the activation of the JAK2/STAT3 pathway in different pain models, such as in animals with a spinal nerve injury. Second, the ob/ob mice were leptin-deficient, but the effect of leptin is enhanced in other research. Third, compared with the animals used in these experiments, the ob/ob mice exhibited complicated physiological conditions, including hyperglycemia and hyperinsulinemia.

We observed that along with progressive mechanical hyperalgesia from 8 to 16 weeks, the JAK2/STAT3 pathway was activated in the spinal dorsal horn of ob/ob mice. Evidence indicated that the JAK2/STAT3 pathway could regulate the expressions and functions of several neurotransmitter receptors, including γ-aminobutyric acid A receptor (GABAAR) and N-methyl-D-aspartate receptor 1 (NMDAR1), thus contributing to neuropathic pain (28,29). In addition, the JAK2/STAT3 pathway acts as downstream effectors of cytokine receptors, including cytokine receptors, growth-hormone like receptors, and the leptin receptor (LepR) (17,30-32). Moreover, long-term hyperinsulinemia exacerbates the inflam-

matory response (33-35). Because the ob/ob mice were leptin-deficient but lepR reserved, the activated JAK2/STAT3 pathway might be due to interleukin-6 (IL-6), which was increased in the T2DM (36,37).

However, in STZ-induced diabetes, the JAK2/STAT3 pathway was inactivated, although this type of diabetic animal exhibited hyperglycemia and mechanical hyperalgesia, implicating a different mechanism of PDN between T1DM and T2DM via the JAK2/STAT3 pathway. We noted that, in contrast to STZ-induced diabetes, there were several mechanisms which could affect PDN of ob/ob mice, including hyperglycemia and hyperinsulinemia. Previous evidence supported that impaired verbal memory in type 2 diabetic patients was associated with hyperinsulinemia but not chronic hyperglycemia (38). Thus, rather than hyperglycemia, hyperinsulinemia in ob/ob mice may exert a major effect on impairing insulin signaling and the activated JAK2/STAT3 pathway in the spinal dorsal horn related to PDN.

Having determined the alternations of insulin signaling and the JAK2/STAT3 pathway *in vivo*, we next did *in vitro* cell cultures and stimulations. Our results further identified the influence of chronic hyperinsulinemia but not hyperglycemia on insulin signaling impairment and the activated JAK2/STAT3 pathway. The cross-talk mechanisms have been demonstrated, thus one possibility is that the insulin-induced mitogen-activated protein kinase (MAPK) phosphorylation may cause the activation of a phosphatase, such as SH2-domain-containing tyrosine phosphatase 2 (SHP-2), which is activated by lepR through JAK2 and able to dephosphorylate IRS-1 (32,39). Taken together, we obtained supportive evidence for the major role of hyperinsulinemia in the 2 signaling pathways, indicating a specific mechanism is involved in PDN of the T2DM.

Finally, we found that the suppressing of the JAK2/STAT3 pathway by AG490 in the spinal cord led to a recovery of mechanical hyperalgesia in ob/ob mice. Although the anti-nociceptive effect of AG490 has been reported (26,27,40), our results supported that AG490 alleviated PDN effectively in the spinal cord. Another important finding was that, after inhibition of the JAK2/STAT3 pathway, the diminished insulin signaling was attenuated. Thus, a role for increased JAK2/STAT3 activity in the regulation of insulin signaling is possible for PDN in ob/ob mice. However, the identification of factors that are responsible for the interaction between insulin signaling and the JAK2/STAT3 pathway in the spinal dorsal horn is another important issue that needs to be investigated in future studies.

Conclusion

In summary, our findings suggest that insulin signaling impairment is associated with an activated JAK2/STAT3 pathway in the spinal dorsal horn. It may contribute to PDN in T2DM. It is also of great interest that the JAK2/STAT3 pathway may serve as a target for pharmacological modification for treating PDN in the T2DM.

Acknowledgement

References

1. Ziegler D. Painful diabetic neuropathy: Treatment and future aspects. *Diabetes Metab Res Rev* 2008; 24: S52-S57.

2. Obrosova IG. Diabetic painful and insensate neuropathy: Pathogenesis and potential treatments. *Neurotherapeutics* 2009; 6:638-647.

3. Fischer TZ, Waxman SG. Neuropathic pain in diabetes--evidence for a central mechanism. *Nat Rev Neurol* 2010; 6:462-466.

4. Drel VR, Mashtalir N, Ilnytska O, Shin J, Li F, Lyzogubov VV, Obrosova IG. The leptin-deficient (ob/ob) mouse: A new animal model of peripheral neuropathy of type 2 diabetes and obesity. *Diabetes* 2006; 55:3335-3343.

5. Daousi C, Benbow SJ, Woodward A, MacFarlane IA. The natural history of chronic painful peripheral neuropathy in a community diabetes population. *Diabet Med* 2006; 23:1021-1024.

6. Eaton SE, Harris ND, Rajbhandari SM, Greenwood P, Wilkinson ID, Ward JD, Griffiths PD, Tesfaye S. Spinal-cord involvement in diabetic peripheral neuropathy. *Lancet* 2001; 358:35-36.

7. Todd AJ. Neuronal circuitry for pain processing in the dorsal horn. *Nat Rev Neurosci* 2010; 11:823-836.

8. Baskin DG, Figlewicz DP, Woods SC, Porte D, Jr., Dorsa DM. Insulin in the brain. *Annu Rev Physiol* 1987; 49:335-347.

9. Unger JW, Livingston JN, Moss AM. Insulin receptors in the central nervous system: Localization, signalling mechanisms and functional aspects. *Prog Neurobiol* 1991; 36:343-362.

10. Greenwood CE, Winocur G. Glucose treatment reduces memory deficits in young adult rats fed high-fat diets. *Neurobiol Learn Mem* 2001; 75:179-189.

11. Lam CK, Chari M, Lam TK. CNS regulation of glucose homeostasis. *Physiology (Bethesda)* 2009; 24:159-170.

12. Bates SH, Myers MG. The role of leptin->STAT3 signaling in neuroendocrine function: An integrative perspective. *J Mol Med (Berl)* 2004; 82:12-20.

13. Bjorbaek C, Kahn BB. Leptin signaling in the central nervous system and the periphery. *Recent Prog Horm Res* 2004; 59:305-331.

14. Fukushima A, Loh K, Galic S, Fam B, Shields B, Wiede F, Tremblay ML, Watt MJ, Andrikopoulos S, Tiganis T. T-cell protein tyrosine phosphatase attenuates STAT3 and insulin signaling in the liver to regulate gluconeogenesis. *Diabetes* 2010; 59:1906-1914.

15. Ortiz-Munoz G, Lopez-Parra V, Lopez-Franco O, Fernandez-Vizarra P, Mallavia B, Flores C, Sanz A, Blanco J, Mezzano S, Ortiz A, Egido J, Gomez-Guerrero C. Suppressors of cytokine signaling abrogate diabetic nephropathy. *J Am Soc Nephrol* 2010; 21:763-772.

16. Marrero MB, Lucas R, Salet C, Hauser TA, Mazurov A, Lippiello PM, Bencherif M. An alpha7 nicotinic acetylcholine receptor-selective agonist reduces weight gain and metabolic changes in a mouse model of diabetes. *The Journal of Pharmacology and Experimental Therapeutics* 2010; 332:173-180.

17. Nicolas CS, Peineau S, Amici M, Csaba Z, Fafouri A, Javalet C, Collett VJ, Hildebrandt L, Seaton G, Choi SL, Sim SE, Bradley C, Lee K, Zhuo M, Kaang BK, Gressens P, Dournaud P, Fitzjohn SM, Bortolotto ZA, Cho K, Collingridge GL. The Jak/STAT pathway is involved in synaptic plasticity. *Neuron* 2012; 73:374-390.

18. Dziennis S, Alkayed NJ. Role of signal transducer and activator of transcription 3 in neuronal survival and regeneration. *Reviews in the Neurosciences* 2008; 19:341-361.

19. Ge SN, Ma YF, Hioki H, Wei YY, Kaneko T, Mizuno N, Gao GD, Li JL. Coexpression of VGLUT1 and VGLUT2 in trigeminothalamic projection neurons in the principal sensory trigeminal nucleus of the rat. *J Comp Neurol* 2010; 518:3149-3168.

20. Brussee V, Guo G, Dong Y, Cheng C, Martinez JA, Smith D, Glazner GW, Fernyhough P, Zochodne DW. Distal degenerative sensory neuropathy in a long-term type 2 diabetes rat model. *Diabetes* 2008; 57:1664-1673.

21. Corkey BE. Banting lecture 2011: Hyperinsulinemia: Cause or consequence? *Diabetes* 2012; 61:4-13.

22. Folli F, Bonfanti L, Renard E, Kahn CR, Merighi A. Insulin receptor substrate-1 (IRS-1) distribution in the rat central nervous system. *J Neurosci* 1994; 14:6412-6422.

23. Araki E, Lipes MA, Patti ME, Bruning JC, Haag B, 3rd, Johnson RS, Kahn CR. Alternative pathway of insulin signalling in mice with targeted disruption of the IRS-1 gene. *Nature* 1994; 372:186-190.

24. Carvalheira JB, Torsoni MA, Ueno M, Amaral ME, Araujo EP, Velloso LA, Gontijo JA, Saad MJ. Cross-talk between the insulin and leptin signaling systems in rat hypothalamus. *Obesity Research*

2005; 13:48-57.

25. Benomar Y, Roy AF, Aubourg A, Djiane J, Taouis M. Cross down-regulation of leptin and insulin receptor expression and signalling in a human neuronal cell line. *Biochem J* 2005; 388:929-939.

26. Dominguez E, Rivat C, Pommier B, Mauborgne A, Pohl M. JAK/STAT3 pathway is activated in spinal cord microglia after peripheral nerve injury and contributes to neuropathic pain development in rat. *Journal of Neurochemistry* 2008; 107:50-60.

27. Tsuda M, Kohro Y, Yano T, Tsujikawa T, Kitano J, Tozaki-Saitoh H, Koyanagi S, Ohdo S, Ji RR, Salter MW, Inoue K. JAK-STAT3 pathway regulates spinal astrocyte proliferation and neuropathic pain maintenance in rats. *Brain* 2011; 134:1127-1139.

28. Lim G, Wang S, Zhang Y, Tian Y, Mao J. Spinal leptin contributes to the pathogenesis of neuropathic pain in rodents. *J Clin Invest* 2009; 119:295-304.

29. Lund IV, Hu Y, Raol YH, Benham RS, Faris R, Russek SJ, Brooks-Kayal AR. BDNF selectively regulates GABAA receptor transcription by activation of the JAK/STAT pathway. *Sci Signal* 2008; 1:ra9.

30. Kim YD, Kim YH, Cho YM, Kim DK, Ahn SW, Lee JM, Chanda D, Shong M, Lee CH, Choi HS. Metformin ameliorates IL-6-induced hepatic insulin resistance via induction of orphan nuclear receptor small heterodimer partner (SHP) in mouse models. *Diabetologia* 2012.;55:1482-1494.

31. Parganas E, Wang D, Stravopodis D, Topham DJ, Marine JC, Teglund S, Vanin EF, Bodner S, Colamonici OR, van Deursen JM, Grosveld G, Ihle JN. Jak2 is essential for signaling through a variety of cytokine receptors. *Cell* 1998; 93:385-395.

32. Li C, Friedman JM. Leptin receptor activation of SH2 domain containing protein tyrosine phosphatase 2 modulates Ob receptor signal transduction. *Proceedings of the National Academy of Sciences of the United States of America* 1999; 96:9677-9682.

33. Valentini L, Wirth EK, Schweizer U, Hengstermann S, Schaper L, Koernicke T, Dietz E, Norman K, Buning C, Winklhofer-Roob BM, Lochs H, Ockenga J. Circulating adipokines and the protective effects of hyperinsulinemia in inflammatory bowel disease. *Nutrition* 2009; 25:172-181.

34. Krogh-Madsen R, Moller K, Dela F, Kronborg G, Jauffred S, Pedersen BK. Effect of hyperglycemia and hyperinsulinemia on the response of IL-6, TNF-alpha, and FFAs to low-dose endotoxemia in humans. *American Journal of Physiology Endocrinology and Metabolism* 2004; 286:E766-E772.

35. Fernandez-Real JM, Pickup JC. Innate immunity, insulin resistance and type 2 diabetes. *Diabetologia* 2012; 55:273-278.

36. Pickup JC, Chusney GD, Thomas SM, Burt D. Plasma interleukin-6, tumour necrosis factor alpha and blood cytokine production in type 2 diabetes. *Life Sciences* 2000; 67:291-300.

37. Pradhan AD, Manson JE, Rifai N, Buring JE, Ridker PM. C-reactive protein, interleukin 6, and risk of developing type 2 diabetes mellitus. *JAMA* 2001; 286:327-334.

38. Vanhanen M, Koivisto K, Kuusisto J, Mykkanen L, Helkala EL, Hanninen T, Riekkinen P Sr, Soininen H, Laakso M. Cognitive function in an elderly population with persistent impaired glucose tolerance. *Diabetes Care* 1998; 21:398-402.

39. Araki T, Nawa H, Neel BG. Tyrosyl phosphorylation of Shp2 is required for normal ERK activation in response to some, but not all, growth factors. *The Journal of Biological Chemistry* 2003; 278:41677-41684.

40. Schweizerhof M, Stosser S, Kurejova M, Njoo C, Gangadharan V, Agarwal N, Schmelz M, Bali KK, Michalski CW, Brugger S, Dickenson A, Simone DA, Kuner R. Hematopoietic colony-stimulating factors mediate tumor-nerve interactions and bone cancer pain. *Nature Medicine* 2009; 15:802-807.